Astronomy & Astrophysics manuscript no. astro3797 February 5, 2008
(DOI: will be inserted by hand later)

High-frequency radio observations of the Kühr sample and the epoch-dependent luminosity function of flat-spectrum quasars

R. Ricci[1,2], I. Prandoni[3], C. Gruppioni[4], R.J. Sault[2], and G. De Zotti[5,1]

[1] SISSA/ISAS, Via Beirut 2–4, I-34014 Trieste, Italy

[2] Australia Telescope National Facility, CSIRO, P.O. Box 76, Epping, NSW 2121, Australia
e-mail: Roberto.Ricci@atnf.csiro.au

[3] INAF, Istituto di Radioastronomia, Via Gobetti 101, I–40129, Bologna, Italy

[4] INAF, Osservatorio Astronomico di Bologna, Via Ranzani 1, I–40126 Bologna, Italy

[5] INAF, Osservatorio Astronomico di Padova, Vicolo dell'Osservatorio 5, I–35122 Padova, Italy
e-mail: dezotti@pd.astro.it

Received ..... ; accepted .....

Abstract. We discuss our ATCA 18.5 and 22 GHz flux density measurements of Southern extragalactic sources in the complete 5 GHz sample of Kühr et al. (1981). The high frequency (5–18.5 GHz) spectral indices of steep-spectrum sources for which we have 18.5 GHz data (66% of the complete sample) are systematically steeper than the low frequency (2.7–5 GHz) ones, with median $\alpha_{2.7}^{5} = 0.76$, median $\alpha_{5}^{18.5} = 1.18$ ($S_\nu \propto \nu^{-\alpha}$), and median steepening $\Delta\alpha = 0.32$, and there is evidence of an anti-correlation of $\Delta\alpha_{5}^{18.5}$ with luminosity. The completeness of 18.5 GHz data is much higher (89%) for flat-spectrum sources (mostly quasars), which also exhibit a spectral steepening: median $\alpha_{2.7}^{5} = -0.14$, median $\alpha_{5}^{18.5} = 0.16$ ($S_\nu \propto \nu^{-\alpha}$), and median $\Delta\alpha = 0.19$. Taking advantage of the almost complete redshift information on flat-spectrum quasars, we have estimated their 5 GHz luminosity function in several redshift bins. The results confirm that their radio luminosity density peaks at $z_{\rm peak} \simeq 2.5$ but do not provide evidence for deviations from pure luminosity evolution as hinted at by other data sets. A comparison of our 22 GHz flux densities with WMAP K-band data for flat-spectrum sources suggests that WMAP flux densities may be low by a median factor of $\simeq 1.2$. The extrapolations of 5 GHz counts and luminosity functions of flat-spectrum radio quasars using the observed distribution of the 5–18.5 spectral indices match those derived directly from WMAP data, indicating that the high frequency WMAP survey does not detect any large population of FSRQs with anomalous spectra.

Key words. radio continuum: galaxies – galaxies: nuclei – quasars: general – luminosity function: radio

1. Introduction

High radio frequency (10-100 GHz) sky surveys have started to become feasible only very recently. The first all-sky surveys at high radio frequencies have been provided by the WMAP satellite (Bennett et al. 2003). In particular, the complete sample of extragalactic sources drawn from its K-band catalog ($S \geq 1.25$ Jy, $|b| \geq 10^\circ$; see De Zotti et al. 2005) comprises 155 extragalactic sources (plus a planetary nebula), over an area of 10.4 sr.

Another survey which which will give a significant contribution to the knowledge of the > 10 GHz extragalactic sky is the ongoing all-sky 20 GHz survey which is being undertaken with the Australia Telescope Compact Array (ATCA) in the Southern emisphere (a pilot survey covers about 1200 deg^2 to 100 mJy, Ricci et al. 2004b).

An example of a deeper survey is the 9th Cambridge survey carried out at 15 GHz with the Ryle Telescope (Waldram et al. 2003), which covers 520 deg^2 to $S = 25$ mJy, and reaches deeper flux densities on smaller areas.

Such surveys are of fundamental importance to directly provide information about the extragalactic populations dominating the sky at > 10 GHz frequencies, and allow to test extrapolated models based mainly on lower frequency selected samples.

In this paper we present 18.5 and 22 GHz observations of the Southern extragalactic sources of the complete 5 GHz sample of Kühr et al. (1981), with the aim of better modeling the high frequency properties of radio galaxies

Send offprint requests to: R. Ricci

and quasars, and check whether radio sources detected by WMAP in the K-band significantly differ from the ones dominating at lower frequencies.

In Sect. 2 we briefly present the 18.5 and 22 GHz flux density measurements. The main high frequency properties of Southern Kühr sources are analysed in Sect. 3. In Sect. 4 we estimate the 5 GHz luminosity function (LF) of FSRQs at different cosmic epochs and compare it with predictions of a recent model by De Zotti et al. (2005). The observed 5–18.5 GHz spectral index distribution is then exploited to extrapolate the LF to 22.8 GHz, the central frequency of the WMAP K-band. The extrapolated LF is compared with a direct estimate from the WMAP data. In Sect. 5 we summarize our main conclusions.

Throughout this paper we adopt a flat Λ cosmology with $\Omega_\Lambda = 0.7$ and $H_0 = 70\,\mathrm{km\,s^{-1}\,Mpc^{-1}}$.

2. The data

In March 2002 we have carried out total intensity and linear polarization measurements at 18.5 GHz of 249 of the 258 southern ($\delta < 0°$) extragalactic sources in the 5 GHz all-sky 1 Jy sample (Kühr et al. 1981; Stickel et al. 1994) with the Australia Telescope Compact Array (ATCA), using the prototype high-frequency receivers mounted on antennas CA02, CA03, and CA04. The array configuration was quite compact, giving a HPBW = 15″.6. Full details on observations and data reduction are provided by Ricci et al. (2004a, hereafter referred to as Paper I), who carried out an analysis of linear polarization data. Many of these sources had already been targeted with the ATCA as part of a search for potential 22 GHz calibrators. The remaining 22 GHz total intensity measurements were taken with ATCA in January 2001 using the three antennas of the 750C array configuration providing a HPBW = 7″.0.

The 18.5 and 22 GHz flux densities are listed in Table 1, where, for each observed source, we also report the 5 GHz flux density, the spectral index between 2.7 and 5 GHz (both from Kühr et al. 1981), the source type (from Stickel et al. 1994) and the source redshift (mostly from Stickel et al. 1994, with some additional redshifts from the NED database).

Both 18.5 and 22 GHz data were reduced as discussed in Paper I. In particular, flux densities are derived using non-imaging model-fitting techniques, which assume a point source model. We notice that the 22 GHz data have larger uncertainties, are less homogeneous and, having better angular resolution, can suffer more from resolution effects. Therefore, our analysis mostly relies on 18.5 GHz data.

Whenever a source at 18.5 GHz is poorly modeled as a point source (see Paper I for details), such source is labeled "R" (for "resolved") in the last column of Table 1, and excluded from further analysis.

Small differences with the 18.5 GHz flux densities, and associated errors, reported by Ricci et al. (Paper I), are due to a new analysis of the measurements. The 18.5 GHz errors now include the flux calibration uncertainty of 5%. Calibration errors, estimated at 10%, are also included in the 22-GHz data.

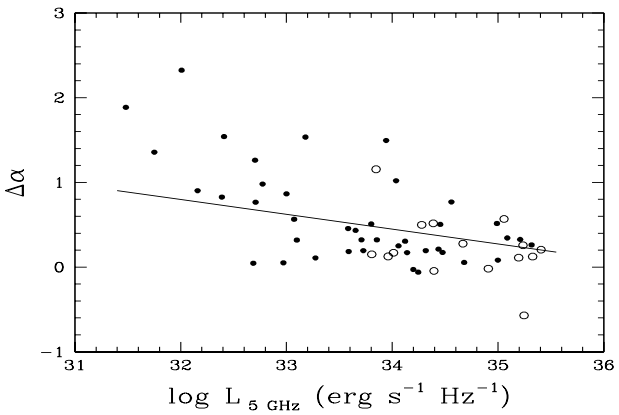

Fig. 1. High-frequency steepening of steep-spectrum sources as a function of the 5 GHz luminosity. Radio galaxies and quasars are indicated by filled and empty circles respectively. The regression line is $\Delta\alpha = -0.1749 \log L_{5\mathrm{GHz}} + 6.3948$.

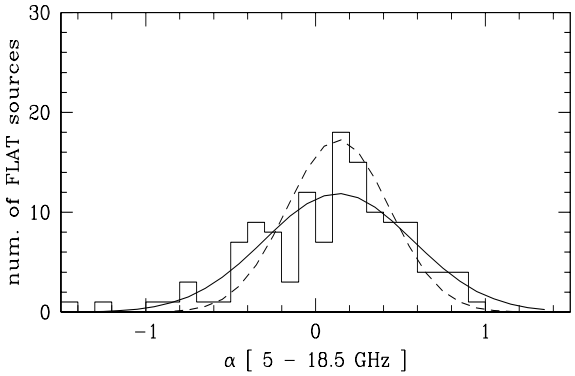

Fig. 2. Distribution of 5–18.5 GHz spectral indices, $\alpha_5^{18.5}$, of flat-spectrum sources in the Kühr sample. The solid line shows the formal best-fit Gaussian representation of the distribution ($<\alpha>= 0.134$, $\sigma = 0.437$), the dashed line is a Gaussian with the same $<\alpha>$ and $\sigma = 0.30$ (see text).

Following Stickel et al. (1994), we have classified as flat-spectrum, sources with 2.7–5 GHz spectral index $\alpha_{2.7}^5 < 0.5$ ($S_\nu \propto \nu^{-\alpha}$); sources with larger values of $\alpha_{2.7}^5$ are classified as steep-spectrum. Of the 249 sources observed, 146 are flat-spectrum and 103 are steep-spectrum.

In the following analysis we exclude "resolved" ("R") sources. This means 130 out of the 146 flat-spectrum sources in the original complete sample (89%) and 68 of the 103 steep-spectrum sources (66%) are retained. Special emphasis will be given to Flat-Spectrum Radio Quasars (FSRQs), which constitute the population which is best represented in our sample.

3. Data analysis

Since the high frequency information on steep-spectrum sources is seriously incomplete (see above), and, as a consequence, any conclusion on their spectral properties may be biased, we only note that they show evidence of a spectral steepening. The median $\alpha_{2.7}^{5}$ is 0.76 ($S_\nu \propto \nu^{-\alpha}$) (the mean is 0.81 ± 0.02), while the median $\alpha_{5}^{18.5}$ is 1.18 (mean 1.28 ± 0.06), and the median steepening is $\Delta\alpha = 0.32$ (mean 0.47 ± 0.06). The steepening is anti-correlated with luminosity (see Fig. 1) or redshift (the Spearman's rank correlation coefficient yields a probability of no correlation of 3×10^{-4}). This translates into an anti-correlation of $\alpha_{5}^{18.5}$ with luminosity (or z), possibly reversing the *positive* correlation with luminosity of the low frequency spectral index (see, e.g., Dunlop & Peacock 1990). Since low-luminosity (and low z) sources are mostly galaxies, while quasars are high-luminosity (and high z) sources (see Fig. 1), we have larger steepenings for galaxies (median $\Delta\alpha = 0.34$) than for quasars (median $\Delta\alpha = 0.20$).

A high-frequency steepening is also observed for flat-spectrum sources, which are mostly FSRQs. The median values are $\alpha_{2.7}^{5} = -0.14$ ($S_\nu \propto \nu^{-\alpha}$), $\alpha_{5}^{18.5} = 0.16$, $\Delta\alpha = 0.19$, while the mean values are, respectively, -0.13 ± 0.03, 0.11 ± 0.04, and 0.24 ± 0.05. The best-fit Gaussian distribution of 2.7–5 GHz spectral indices has a mean of -0.10 and a dispersion of 0.30, while that of 5–18.5 GHz spectral indices has mean 0.13 and dispersion 0.44 (Fig. 2). The large value for the dispersion of the distribution of $\alpha_{5}^{18.5}$ may be partly due to measurement errors and to uncertainties in the source classification; we will come back to this in Sect. 4.2. The Spearman's rank correlation statistics detects a *positive* correlation of $\alpha_{5}^{18.5}$ with luminosity (or z), although with a lower significance than for steep-spectrum sources (probability of no correlation 2×10^{-3}).

3.1. Comparison with WMAP K-band flux measurements

It is interesting to compare our 18.5 GHz flux density measurements of flat-spectrum unresolved sources of the Kühr sample with those of WMAP in the K-band (22.8 GHz). A cross-correlation with the WMAP catalog (Bennett et al. 2003) yields 59 matches within angular separations of 11 arcmin (the Bennett et al. 2003 criterion for WMAP source cross-identifications). For the un-matched flat-spectrum sources in our sample we adopt an upper flux density limit in the K-band of $S_K = 1.25$ Jy, i.e. the completeness limit of the WMAP survey, as derived by De Zotti et al. (2005; see also Argüeso et al. 2003). We notice, however, that Bennett et al. (2003) give a less conservative estimate of $S_K = 0.75$ Jy. Using the Kaplan-Meier estimator [routine KMESTM in the software package ASURV Rev 1.2 (Isobe & Feigelson, 1990)] we get an estimated median value of $\log(S_{18.5\mathrm{GHz}}/S_K) = 0.098$ (corresponding to $S_{18.5\mathrm{GHz}}/S_K = 1.25$). This includes WMAP flux density upper limits by implementing the survival analysis methods presented in Feigelson & Nelson (1985) and Isobe, Feigelson & Nelson (1986). The mean value of $\log(S_{18.5\mathrm{GHz}}/S_K)$, $0.126 +/- 0.021$, is less reliable because it is significantly affected by outliers (probably variable sources).

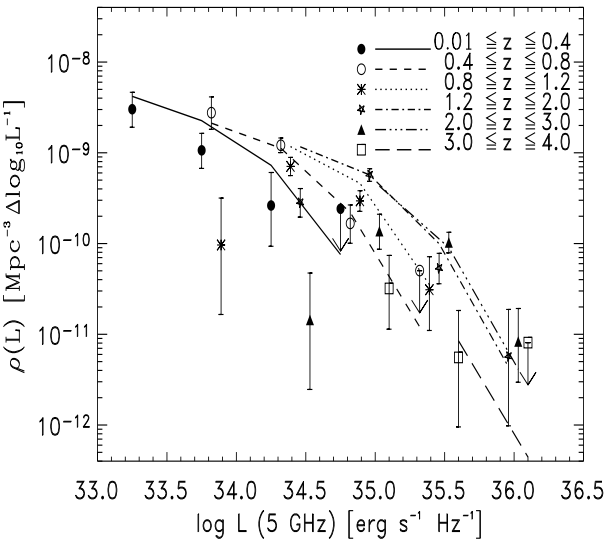

Fig. 3. Comoving luminosity function of FSRQs in the Kühr et al. (1981) sample for different redshift bins (points), compared with the model by De Zotti et al. 2005 (lines).

The median $\alpha_{5}^{18.5} = 0.16$ would imply a significantly lower value ($\log(S_K) = \log(S_{22.8\mathrm{GHz}}) = \log(S_{18.5\mathrm{GHz}}) - 0.16\log(22.8/18.5)$, or $\log(S_{18.5\mathrm{GHz}}/S_K) = 0.015$) and using the actually observed distribution of $\alpha_{5}^{18.5}$ for flat-spectrum sources (see Fig. 2) we obtain an even lower mean value ($\log(S_{18.5\mathrm{GHz}}/S_{22.8\mathrm{GHz}}) = 0.0097 \pm 0.0009$), suggesting that the WMAP K-band flux densities are systematically lower than the ATCA flux densities by a factor of $\simeq 1.2$. Using our measurements at the closer frequency of 22 GHz (which has, however, a larger calibration uncertainty) we find a median value $\log(S_{22\mathrm{GHz}}/S_K) = 0.057$ (mean $\log(S_{22\mathrm{GHz}}/S_K) = 0.101 \pm 0.025$), confirming the indication of a small, but non-negligible offset.

4. The epoch-dependent luminosity function of FSRQs

4.1. The 5 GHz luminosity function

To estimate the epoch-dependent 5 GHz luminosity function of FSRQs we exploit the full Kühr et al. (1981) sample, including the Northern portion, not observed at 18.5 GHz. The redshift information is essentially complete: Stickel et al. (1994) list redshifts for 198 of the 214 FSRQs in that sample and a search in the NASA-IPAC Extragalactic Database (NED) yielded redshift measurements for 8 additional objects. In summary, the redshift completeness is 94% in the flux density bin $0 \leq$

$\log S_5(\mathrm{Jy}) < 0.2$, 98% in the bin $0.2 \leq \log S_5(\mathrm{Jy}) < 0.4$ and 100% at higher flux densities.

We have estimated the 5 GHz luminosity function, averaged over intervals $\Delta \log L = 0.5$, in six redshift bins ($0.01 < z \leq 0.4$, $0.4 < z \leq 0.8$, $0.8 < z \leq 1.2$, $1.2 < z \leq 2$, $2 < z \leq 3$, $3 < z \leq 4$) using the classical $1/V_{\rm max}$ method (Schmidt 1968):

$$\Phi(L_5, z) = \sum_{L_i \in [L_5 - \Delta L/2, L_5 + \Delta L/2]} \frac{w_i}{V_{\rm max,i}} \qquad (1)$$

where $V_{\rm max}$ is the maximum volume accessible to each source and w_i is the weight factor correcting for the redshift incompleteness. $V_{\rm max}$ is given by the integral of the volume element from the lower bound of the redshift bin to $z_{\rm max} = \min(z_{\rm up}, z_{\rm lim})$, where $z_{\rm up}$ is the upper bound of the bin and $z_{\rm lim}$ is the redshift at which the source would have a flux density of 1 Jy (i.e. the lower limit of the Kühr sample). The weight factor w_i is set at $w_i = 1/0.94$ and at $w_i = 1/0.98$, respectively, for sources in the two lowest flux density bins, defined above, and at $w_i = 1$ for brighter sources. The K-correction was computed using the spectral index $\alpha^5_{2.7}$ of each source (see Kühr et al. 1981). The area covered by the catalog is 9.81 sr. The 68% confidence intervals on the luminosity function were computed assuming Poisson statistics with an effective number of sources per bin given by:

$$n_{\rm eff} = \left(\sum_i 1/V_{\rm max,i} \right)^2 / \sum_i 1/V^2_{\rm max,i} \; . \qquad (2)$$

In Fig. 3 the estimated luminosity functions (points) are compared with the model by De Zotti et al. (2005), averaged over the same luminosity and redshift bins (lines). The agreement is generally satisfactory. In spite of its simplicity (it assumes pure luminosity evolution), the model correctly reproduces the positive evolution up to $z \sim 2.5$ and the subsequent negative evolution.

4.2. Extrapolation to high frequencies

We now use the WMAP K-band catalogue to derive the 22.8 GHz luminosity function and compare it to the one extrapolated from 5 GHz. After having multiplied the WMAP fluxes by 1.2 (see Sect. 3), and using the 4.85 GHz flux densities from the GB6 (Gregory et al. 1996) or PMN (available at http://www.parkes.atnf.csiro.au/) catalogs, 143 of them have been classified as flat-spectrum based on the 4.85–22.8 GHz spectral indices ($\alpha^{22.8}_{4.85} < 0.5$, $S_\nu \propto \nu^{-\alpha}$). A search in the NASA/IPAC NED database yielded optical identifications for 122 of the flat-spectrum sources (94 FSRQs and 28 BL Lacs). The 21 objects classified as galaxies or unidentified have been partitioned randomly between FSRQs and BL Lacs, in proportion to the number of identified objects in each class; this procedure has added 16 objects to the FSRQ sample.

In Fig. 4 the K-band differential counts of WMAP FSRQs (points) are compared with the ones extrapolated from the corresponding 5 GHz counts, as described by the De Zotti et al. (2005) model, exploiting the Gaussian representations of the spectral index distribution of Fig. 2. If we adopt the formal best-fit value of the dispersion, $\sigma = 0.44$, we over-predict the WMAP counts (see dashed line in Fig. 4) , confirming that the spectral index distribution is broadened by measurement errors. With $\sigma = 0.30$,

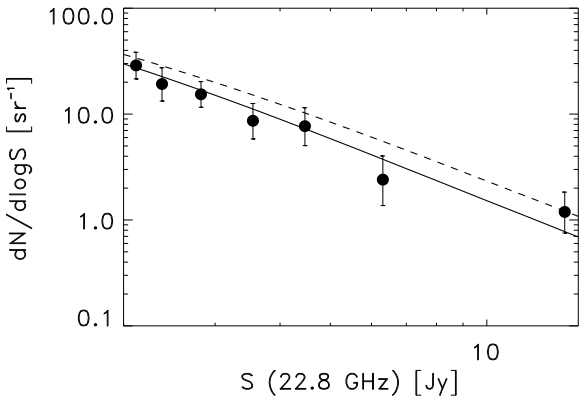

Fig. 4. Differential counts of FSRQs in the complete WMAP K-band sample (see text), compared with the extrapolations of 5 GHz counts using the Gaussian representations of the 5–18.5 GHz spectral index distribution of Fig. 2, namely $< \alpha >= 0.13$ and $\sigma = 0.44$ (dashed line) or $\sigma = 0.30$ (solid line). The WMAP fluxes have been multiplied by 1.2 (see Sect. 3). The error bars show the 68% confidence intervals for Poisson statistics (Gehrels 1986).

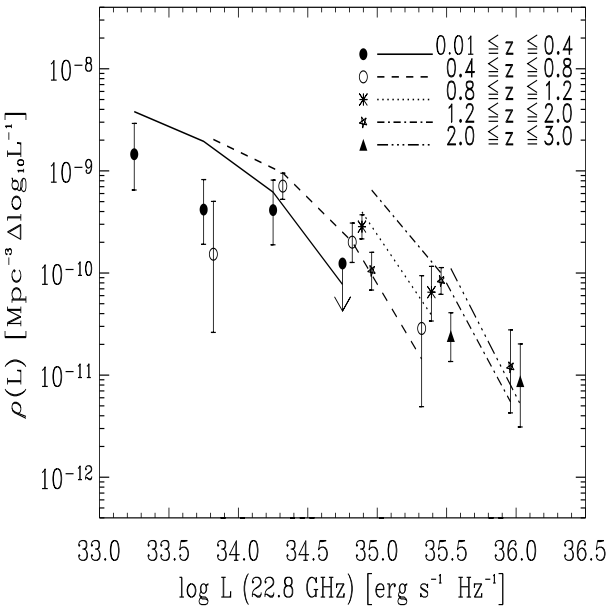

Fig. 5. Comoving luminosity function of FSRQs in the complete WMAP sample (see text) for different redshift bins compared with the model by De Zotti et al. (2005).

close to the dispersion of the 2.7–5 GHz spectral index distribution, the agreement is good (see solid line in Fig. 4), indicating that high frequency surveys do not detect many FSRQs with "anomalous" radio spectra.

Redshift measurements were found in the literature for 99 of the 110 objects in the WMAP FSRQ sample. We have estimated their luminosity function for the same luminosity and redshift bins as for the Kühr sample (see Fig. 3), except for the highest redshift bin, because we have only one WMAP source at $z > 3$. The K-corrections have been computed using the median 4.85–18.5 GHz spectral index $\alpha_{4.85}^{18.5} = 0.16$; this has been preferred to $\alpha_{4.85}^{22.8}$ of individual objects which are too liable to variability. In Fig. 5 these estimates (points) are compared with the extrapolations of the 5 GHz luminosity function as modeled by the De Zotti et al. (2005), which provides a good representation of the data (see lines), when we use the 5–18.5 GHz Gaussian spectral index distribution with $< \alpha >= 0.13$ and $\sigma = 0.30$.

5. Conclusions

The ATCA 18.5 and 22 GHz flux density measurements of Southern extragalactic sources in the complete 5 GHz sample of Kühr et al. (1981) have been analyzed. The non-imaging technique used yielded reliable flux density measurements for 66% of steep-spectrum sources. Although this incompleteness requires caution in dealing with the data, some interesting indications emerge. First the high frequency (5–18.5 GHz) spectral indices are systematically steeper than the low frequency (2.7–5 GHz) ones, the median steepening being $\Delta\alpha = 0.32$. There is a hint of a larger steepening for sources classified as galaxies than for those classified as QSOs. Since QSOs have generally higher luminosities and higher redshifts than galaxies, this difference translates into an anti-correlation of $\Delta\alpha$ with the radio luminosity (or z) when we consider the full steep-spectrum sample. As a consequence, the *positive* correlation of the radio luminosity with the low frequency spectral index (see, e.g., Dunlop & Peacock 1990), seems to *get reversed* when we consider the high frequency spectral index. More complete data would however be necessary to test the reliability of this indication.

The information on 18.5 GHz flux densities of flat-spectrum sources (mostly FSRQs) has a much better completeness level (89%). A high-frequency steepening is again present, with median values $\alpha_{2.7}^{5} = -0.14$, $\alpha_{5}^{18.5} = 0.16$, $\Delta\alpha = 0.19$. Luminosities of these sources are positively correlated, though weakly, with both the low and the high frequency spectral indices.

In addition to having almost complete 18.5 GHz data, FSRQs have almost complete redshift information, that has been exploited to estimate their luminosity function in several redshift bins. The 5 GHz luminosity functions, computed using the full 1 Jy sample, while confirming that the radio luminosity density peaks at $z_{\rm peak} \simeq 2.5$ (Dunlop & Peacock 1990; Shaver et al. 1996, 1999) do not provide evidence for deviations from pure luminosity evolution, reported by other analyses (Hook et al. 1998; Vigotti et al. 2003), perhaps due to the poor statistics. In particular we notice that the derived epoch-dependent 5 GHz luminosity function is fairly well represented by the model by De Zotti et al. (2005).

We exploit the multi-frequency 2.7, 5 and 18.5 GHz information, for Southern Kühr FSRQs to better extrapolate the De Zotti et al. model to 22.8 GHz, i.e. the central frequency of the WMAP K-band survey. This allows us to properly take into account the spectral steepening of FSQRs between 5 and 18.5 GHz.

The extrapolated model is compared to the sample of FSRQs detected in the K-band by WMAP. To this respect, it is interesting to note that a direct comparison between ATCA 18.5/22 GHz and WMAP K-band flux density measurements for flat-spectrum sources hints towards a systematic under-estimation of WMAP fluxes by a factor ~ 1.2.

After correcting the WMAP K-band fluxes for the afore-mentioned offset, we are able to get very good agreement between the differential counts of WMAP K-band FSRQs and the modeled extrapolation to 22.8 GHz. The same happens when we analyze the luminosity properties of the FSRQ WMAP sample. The K-band epoch-dependent luminosity function derived from the sample of WMAP FSRQs is fairly well reproduced by the modeled 5 GHz luminosity function, extrapolated to 22.8 GHz as described above.

Such results imply that the WMAP survey does not detect substantial numbers of FSRQs with anomalous spectra.

Acknowledgements. This research was supported in part by the Italian Space Agency (ASI) and by the Italian MIUR through a COFIN grant. RR warmly thanks the Paul Wild Observatory staff for their kind hospitality at Narrabri (NSW, Australia) where some of this work was accomplished. The Australia Telescope is funded by the Commonwealth of Australia for operation as a National Facility managed by CSIRO. This research has made use of the NASA/IPAC Extragalactic Database (NED) which is operated by the Jet Propulsion Laboratory, California Institute of Technology, under contract with the National Aeronautics and Space Administration.

References

Argüeso, F., González-Nuevo, J., & Toffolatti, L. 2003, ApJ, 598, 86

Bennett, C.L., Hill, R.S., Hinshaw, G., et al. 2003, ApJS, 148, 97

De Zotti, G., Ricci, R., Mesa, D., Silva, L., Mazzotta, P., Toffolatti, L., & González-Nuevo, J. 2005, A&A, 431, 893

Dunlop, J.S. & Peacock, J.A. 1990, MNRAS, 247, 19

Feigelson, E.D., & Nelson, P.I., 1985, ApJ, 293, 192

Gehrels, N. 1986, ApJ, 303, 336

Gregory, P.C., Scott, W.K., Douglas, K., & Condon, J.J. 1996, ApJS, 103, 427

Hook, I.M., Shaver, P.A., & McMahon, R.G. 1998, in *The Young Universe*, ASP Conf. series, S. D'Odorico, A. Fontana, E. Giallongo, eds., Vol. 146, p. 17

Isobe, T., & Feigelson, E.D., 1990, Bull. Amer. Astro. Society, 22, 917
Isobe, T., Feigelson, E.D., & Nelson, P.I., 1986, ApJ, 306, 490
Kühr, H., Witzel, A., Pauliny-Toth, I.I.K., & Nauber, U. 1981, A&AS, 45, 367
Ricci, R., Prandoni, I., Gruppioni, C., Sault, R.J., & De Zotti, G. 2004a, A&A, 415, 549 (Paper I)
Ricci, R., Sadler, E.M., Ekers, R.D., Staveley–Smith, L., Wilson, W.E., Kesteven, M.J., Subrahmanyan, R., Walker, M.A., Jackson, C.A., & De Zotti, G. 2004b, MNRAS, 354, 305
Schmidt, M. 1968, ApJ, 151, 393
Shaver, P.A., Wall, J.V., Kellermann, K.I., Jackson, C.A., & Hawkins, M.R.S. 1996, Natur, 384, 439
Shaver, P.A., Hook, I.M., Jackson, C.A., Wall, J.V., Kellermann, K.I. 1999, in Highly Redshifted Radio Lines, ASP Conf. Series, C.L. Carilli, S.J.E. Radford, K.M. Menten, & G.I. Langston eds., 156, 163
Stickel, M., Meisenheimer, K., & Kühr, H. 1994, A&A Supp. Ser., 105, 211
Vigotti, M., Carballo, R., Benn, C.R., De Zotti, G., Fanti, R., Gonzalez Serrano, J.I., Mack, K.-H., & Holt, J. 2003, ApJ, 591, 43
Waldram, E.M., Pooley, G.G., Grainge, K.J.B., Jones, M.E., Saunders, R.D.E., Scott, P.F., Taylor, A.C., 2003, MNRAS, 342, 915

Table 1. 18.5 and 22 GHz flux density measurements of Southern sources in the Kühr sample. The flag in the last column indicates the reliability of the 18.5 GHz measurements. Also listed are the 5 GHz flux density and the $2.7-5$ GHz spectral index (from Kühr et al. 1981), the source type and redshift (from Stickel et al. 1994, plus some redshifts from NED).

Name	$S_{5\mathrm{GHz}}$ (Jy)	$\alpha^5_{2.7}$	type	z	$S_{18.5\mathrm{GHz}}$ (Jy)	$S_{22\mathrm{GHz}}$ (Jy)	ext
0003-066	1.48	-0.02	QSO	0.3470	2.352 ± 0.118	2.551 ± 0.255	-
0003-003	1.39	0.84	QSO	1.0370	0.474 ± 0.028	0.454 ± 0.045	-
0008-421	1.23	1.14	GAL	0.1716	0.182 ± 0.009	0.134 ± 0.013	-
0022-423	1.83	0.72	QSO	0.9370	0.339 ± 0.017	0.252 ± 0.025	-
0023-263	3.62	0.72	GAL	0.3220	1.129 ± 0.057	1.051 ± 0.105	-
0034-014	1.59	0.73	GAL	0.0730	0.211 ± 0.011	0.176 ± 0.018	R
0035-024	2.69	0.65	GAL	0.2197	0.652 ± 0.035	0.608 ± 0.061	-
0039-445	1.21	0.88	GAL	0.3460	0.197 ± 0.010	0.175 ± 0.018	-
0042-357	1.01	0.79	—	–	0.218 ± 0.011	0.215 ± 0.022	-
0043-424	3.17	0.72	GAL	0.0526	0.165 ± 0.008	0.162 ± 0.016	-
0045-255	2.34	0.74	GAL	0.0009	0.571 ± 0.029	0.489 ± 0.049	-
0047-579	2.40	-0.33	QSO	1.7970	1.647 ± 0.082	1.037 ± 0.104	-
0048-097	1.98	-0.43	BL/QSO	0.1221	1.384 ± 0.069	1.144 ± 0.114	-
0055-016	2.13	0.79	GAL	0.0447	0.108 ± 0.006	0.091 ± 0.009	R
0056-572	1.10	-0.58	QSO	0.0180	0.580 ± 0.029	0.777 ± 0.078	-
0105-163	1.18	1.00	GAL	0.4000	0.084 ± 0.004	0.060 ± 0.006	-
0112-017	1.20	0.01	QSO	1.3810	0.789 ± 0.040	1.186 ± 0.119	-
0113-118	1.94	-0.14	QSO	0.6720	1.419 ± 0.071	1.440 ± 0.144	-
0114-476	2.31	0.60	GAL	0.1460	0.017 ± 0.002	0.030 ± 0.003	R
0114-211	1.28	0.89	GAL	1.4100	0.283 ± 0.014	0.243 ± 0.024	-
0117-155	1.61	0.87	GAL	0.5650	0.267 ± 0.013	0.154 ± 0.015	-
0118-272	1.14	-0.28	BL/QSO	0.5570	0.827 ± 0.042	0.850 ± 0.085	R
0122-003	1.23	0.02	QSO	1.0700	1.728 ± 0.087	1.664 ± 0.166	-
0123-016	1.85	0.83	GAL	0.0177	0.156 ± 0.008	0.154 ± 0.015	R
0130-171	1.00	0.06	QSO	1.0220	1.541 ± 0.078	1.675 ± 0.168	-
0131-522	1.22	-0.18	QSO	0.0200	0.797 ± 0.040	1.045 ± 0.104	-
0131-367	2.23	1.49	GAL	0.0300	0.054 ± 0.003	0.068 ± 0.007	-
0135-247	1.70	-0.35	QSO	0.8310	0.873 ± 0.044	1.705 ± 0.171	R
0138-097	1.22	-0.88	BL/QSO	0.5010	0.929 ± 0.047	1.110 ± 0.111	-
0159-117	1.39	0.59	QSO	0.6690	0.681 ± 0.035	0.772 ± 0.077	-
0201-440	1.04	0.80	QSO?	–	0.257 ± 0.013	0.238 ± 0.024	-
0202-172	1.38	0.03	QSO	1.7400	1.076 ± 0.054	1.523 ± 0.152	-
0208-512	3.31	0.12	QSO	1.0030	2.893 ± 0.145	6.142 ± 0.614	-
0213-132	1.71	0.81	GAL	0.1480	0.183 ± 0.009	0.133 ± 0.013	R
0235-197	1.45	0.83	GAL	0.6200	0.179 ± 0.009	0.160 ± 0.016	-
0237-233	3.40	0.68	QSO	2.2240	0.919 ± 0.046	0.848 ± 0.085	-
0238-084	1.44	-1.19	GAL	0.0050	1.014 ± 0.052	1.622 ± 0.162	-
0240-002	1.80	0.86	GAL	0.0034	0.432 ± 0.022	0.342 ± 0.034	R
0252-712	1.63	1.04	GAL	0.5660	0.317 ± 0.016	0.204 ± 0.020	-
0302-623	1.41	-0.18	QSO	–	1.866 ± 0.093	1.468 ± 0.147	-
0308-611	1.36	-0.76	QSO	–	1.211 ± 0.061	1.141 ± 0.114	-
0319-453	1.02	1.14	GAL	0.0633	0.009 ± 0.002	0.017 ± 0.002	R
0332-403	2.56	-0.43	QSO	1.4450	1.781 ± 0.089	1.631 ± 0.163	-
0336-019	2.86	-0.30	QSO	0.8520	4.062 ± 0.203	3.262 ± 0.326	-
0344-345	1.39	0.68	GAL	0.0538	0.098 ± 0.005	0.040 ± 0.004	R
0349-278	2.34	0.51	GAL	0.0656	0.025 ± 0.002	0.040 ± 0.004	R
0400-319	1.06	0.12	QSO	1.2880	0.876 ± 0.044	0.711 ± 0.071	-
0402-362	1.38	-0.46	QSO	1.4170	3.175 ± 0.159	1.311 ± 0.131	-
0403-132	2.88	0.05	QSO	0.5710	2.281 ± 0.114	2.731 ± 0.273	-
0405-385	1.09	-0.11	QSO	1.2850	1.638 ± 0.082	1.154 ± 0.115	-
0405-123	1.96	0.30	QSO	0.5740	1.413 ± 0.071	1.185 ± 0.118	-
0407-658	3.43	1.13	QSO?	–	0.461 ± 0.023	0.349 ± 0.035	-
0409-752	4.43	0.87	GAL	0.6940	0.906 ± 0.045	0.726 ± 0.073	-
0413-210	1.43	0.29	QSO	0.8070	0.858 ± 0.043	1.195 ± 0.120	-
0414-189	1.35	-0.22	QSO	1.5360	0.904 ± 0.045	0.549 ± 0.055	-

Table 1. Continued.

Name	$S_{5\mathrm{GHz}}$ (Jy)	$\alpha^{5}_{2.7}$	type	z	$S_{18.5\mathrm{GHz}}$ (Jy)	$S_{22\mathrm{GHz}}$ (Jy)	ext
0420-014	1.46	-0.01	QSO	0.9150	7.931 ± 0.397	7.111 ± 0.711	-
0426-380	1.17	-0.20	BL/QSO	1.0300	1.053 ± 0.053	1.206 ± 0.121	-
0427-539	2.32	0.54	GAL	0.0390	0.055 ± 0.003	0.043 ± 0.004	-
0434-188	1.23	-0.25	QSO	2.7020	0.424 ± 0.021	0.436 ± 0.044	-
0437-454	1.41	-0.24	QSO	–	1.124 ± 0.056	1.088 ± 0.109	-
0438-436	6.94	-0.25	QSO	2.8520	3.896 ± 0.195	3.512 ± 0.351	-
0440-003	2.61	0.29	QSO	0.8440	1.215 ± 0.061	1.408 ± 0.141	-
0442-282	2.20	0.89	GAL	0.1470	0.086 ± 0.006	0.286 ± 0.029	R
0454-810	1.40	-0.29	QSO	0.4440	1.565 ± 0.078	2.033 ± 0.203	-
0451-282	2.26	0.04	QSO	2.5590	1.747 ± 0.087	2.565 ± 0.257	-
0453-206	1.84	0.70	GAL	0.0354	0.158 ± 0.008	0.106 ± 0.011	R
0454-463	2.32	0.03	QSO	0.8580	3.585 ± 0.179	2.532 ± 0.253	-
0454-234	2.06	-0.16	QSO	1.0030	5.401 ± 0.270	2.495 ± 0.249	-
0458-020	1.74	0.08	QSO	2.2860	1.570 ± 0.079	1.224 ± 0.122	-
0506-612	1.73	0.10	QSO	1.0930	2.455 ± 0.123	2.742 ± 0.274	-
0511-484	1.81	0.63	GAL	0.3063	0.068 ± 0.004	0.100 ± 0.010	R
0511-220	1.31	-0.13	QSO	1.2960	0.768 ± 0.039	0.603 ± 0.060	-
0514-459	1.06	0.32	QSO	0.1940	0.887 ± 0.044	1.156 ± 0.116	-
0518-458	15.45	1.02	GAL	0.0342	0.780 ± 0.039	1.096 ± 0.110	-
0521-365	9.29	0.43	GAL	0.0550	2.777 ± 0.139	3.971 ± 0.397	R
0524-460	1.02	-0.14	QSO	1.4790	0.524 ± 0.026	0.779 ± 0.078	-
0528-250	1.16	0.20	QSO	2.7650	0.468 ± 0.024	0.390 ± 0.039	-
0537-441	4.00	-0.06	BL/QSO	0.8960	10.667 ± 0.533	9.031 ± 0.903	-
0537-286	1.02	-0.52	QSO	3.1190	0.865 ± 0.043	1.639 ± 0.164	-
0539-057	1.55	-1.41	QSO	0.8390	0.757 ± 0.038	0.913 ± 0.091	-
0602-319	1.25	0.67	QSO	0.4520	0.417 ± 0.021	0.262 ± 0.026	-
0604-203	1.04	0.89	GAL	0.1640	0.105 ± 0.006	0.061 ± 0.006	-
0605-085	3.49	-0.09	QSO	0.8720	1.930 ± 0.097	2.456 ± 0.246	-
0606-223	1.40	-0.55	QSO	1.9260	0.951 ± 0.048	0.896 ± 0.090	-
0607-157	1.82	0.01	QSO	0.3240	5.991 ± 0.300	5.451 ± 0.545	-
0614-349	1.37	0.58	GAL	0.3290	0.497 ± 0.025	0.433 ± 0.043	-
0618-371	1.37	0.40	GAL	0.0326	0.024 ± 0.005	0.035 ± 0.004	R
0620-526	1.27	0.79	GAL	0.0511	0.243 ± 0.012	0.176 ± 0.018	R
0625-536	1.86	1.12	GAL	0.0540	0.077 ± 0.004	0.080 ± 0.008	R
0625-354	2.20	0.45	GAL	0.0550	1.097 ± 0.055	0.792 ± 0.079	R
0637-752	5.85	-0.19	QSO	0.6540	4.780 ± 0.239	4.118 ± 0.412	-
0642-349	1.02	-0.13	QSO	2.1650	0.322 ± 0.016	0.352 ± 0.035	-
0743-673	1.79	0.69	QSO	1.5110	1.556 ± 0.078	1.384 ± 0.138	R
0743-006	1.99	-0.57	QSO	0.9940	1.614 ± 0.081	1.317 ± 0.132	-
0805-077	1.04	0.32	QSO	1.8370	1.661 ± 0.083	2.288 ± 0.229	-
0806-103	1.64	0.67	GAL	0.1070	0.189 ± 0.010	0.308 ± 0.031	-
0825-202	1.18	0.93	QSO	0.8220	0.217 ± 0.011	0.361 ± 0.036	R
0834-201	3.72	-0.03	QSO	2.7520	4.353 ± 0.218	1.982 ± 0.198	-
0834-196	1.52	0.92	GAL?	1.0320	0.410 ± 0.021	0.444 ± 0.044	-
0842-754	1.42	0.67	QSO	0.5240	0.308 ± 0.016	0.509 ± 0.051	-
0858-279	1.42	0.55	QSO	2.1520	1.459 ± 0.073	1.247 ± 0.125	-
0859-257	1.74	0.92	GAL	0.3050	0.182 ± 0.009	0.343 ± 0.034	R
0859-140	2.30	0.42	QSO	1.3390	1.190 ± 0.060	1.334 ± 0.133	-
0915-118	13.99	0.86	GAL	0.0547	2.169 ± 0.109	1.803 ± 0.180	-
0919-260	1.32	-0.22	QSO	2.3000	1.441 ± 0.072	1.441 ± 0.144	-
0941-080	1.09	0.72	GAL	0.2280	0.369 ± 0.019	0.425 ± 0.043	-
1015-314	1.40	0.75	QSO	1.3460	0.454 ± 0.023	0.437 ± 0.044	-
1017-426	1.27	0.98	QSO	1.2800	0.251 ± 0.013	0.177 ± 0.018	-
1032-199	1.15	-0.07	QSO	2.1980	1.261 ± 0.063	1.282 ± 0.128	-
1045-188	1.14	-0.32	QSO	0.5950	1.626 ± 0.081	2.966 ± 0.297	-
1046-409	1.07	0.41	QSO	0.6200	0.413 ± 0.021	0.418 ± 0.042	R
1057-797	1.62	-0.58	QSO	–	2.561 ± 0.128	2.286 ± 0.229	-

Table 1. Continued.

Name	$S_{5\mathrm{GHz}}$ (Jy)	$\alpha^5_{2.7}$	type	z	$S_{18.5\mathrm{GHz}}$ (Jy)	$S_{22\mathrm{GHz}}$ (Jy)	ext
1104-445	2.07	-0.16	QSO	1.5980	2.278 ± 0.114	3.040 ± 0.304	-
1116-462	1.35	0.35	QSO	0.7130	0.959 ± 0.048	0.911 ± 0.091	-
1127-145	6.57	-0.03	QSO	1.1870	2.926 ± 0.146	3.099 ± 0.310	-
1136-135	2.11	0.42	QSO	0.5540	0.434 ± 0.022	0.430 ± 0.043	R
1143-483	1.23	0.64	GAL	0.2982	0.418 ± 0.021	0.612 ± 0.061	-
1143-245	1.18	0.18	QSO	1.9500	0.692 ± 0.035	0.620 ± 0.062	-
1144-379	1.61	-0.66	BL/QSO	1.0480	4.433 ± 0.222	3.193 ± 0.319	-
1145-071	1.25	-0.22	QSO	1.3420	0.811 ± 0.041	0.541 ± 0.054	-
1148-001	1.90	0.44	QSO	1.9820	0.964 ± 0.048	0.880 ± 0.088	-
1151-348	2.83	0.65	QSO	0.2580	0.992 ± 0.050	0.857 ± 0.086	-
1202-262	1.04	0.41	QSO	0.7890	0.514 ± 0.026	0.506 ± 0.051	-
1213-172	1.47	-0.05	GAL	0.6691	1.897 ± 0.095	2.068 ± 0.207	-
1221-423	1.03	0.76	GAL	0.1706	0.357 ± 0.018	0.347 ± 0.035	-
1229-021	1.07	0.29	QSO	1.0450	0.676 ± 0.034	0.492 ± 0.049	-
1237-101	1.31	0.25	QSO	0.7530	1.035 ± 0.052	1.014 ± 0.101	-
1239-044	1.01	1.05	GAL	0.4800	0.184 ± 0.009	0.290 ± 0.029	-
1243-072	1.03	-0.44	QSO	1.2860	0.700 ± 0.035	0.608 ± 0.061	-
1244-255	1.36	-0.30	QSO	0.6330	1.848 ± 0.093	1.416 ± 0.142	-
1245-197	2.50	0.70	QSO	1.2750	0.764 ± 0.038	0.593 ± 0.059	-
1246-410	1.38	0.77	GAL	0.0093	0.213 ± 0.011	0.206 ± 0.021	-
1251-122	2.76	0.83	GAL	0.0145	0.032 ± 0.002	0.081 ± 0.008	R
1253-055	14.95	-0.30	QSO	0.5360	27.946 ± 1.397	20.602 ± 2.060	-
1255-316	1.73	-0.24	QSO	1.9240	1.996 ± 0.100	1.377 ± 0.138	-
1302-102	1.17	-0.17	QSO	0.2860	0.820 ± 0.041	0.969 ± 0.097	-
1306-095	1.94	0.68	GAL?	0.4640	0.827 ± 0.042	0.696 ± 0.070	-
1308-220	1.16	1.23	GAL	0.8000	0.216 ± 0.011	0.284 ± 0.028	-
1313-333	1.36	-0.50	QSO	1.2100	1.457 ± 0.073	4.031 ± 0.403	-
1318-434	2.02	0.69	GAL	0.0110	0.534 ± 0.027	0.569 ± 0.057	-
1320-446	1.07	0.83	QSO	–	0.283 ± 0.014	0.236 ± 0.024	-
1322-428	3.00	0.35	GAL	0.0016	6.479 ± 0.324	6.631 ± 0.663	-
1331-098	1.33	0.60	GAL	0.0810	0.068 ± 0.006	0.472 ± 0.047	R
1333-337	6.90	0.60	GAL	0.0129	0.267 ± 0.013	0.349 ± 0.035	-
1334-127	2.24	-0.17	QSO	0.5390	7.036 ± 0.352	11.007 ± 1.101	-
1335-061	1.02	0.95	QSO	0.6250	0.150 ± 0.008	0.271 ± 0.027	-
1352-104	1.01	-0.40	QSO	0.3320	1.623 ± 0.081	0.913 ± 0.091	-
1354-152	1.52	0.10	QSO	1.8900	0.998 ± 0.050	1.126 ± 0.113	-
1355-416	1.44	0.88	QSO	0.3130	0.101 ± 0.005	0.135 ± 0.014	-
1406-076	1.08	-0.19	QSO	1.4940	1.771 ± 0.089	1.170 ± 0.117	-
1424-418	3.13	-0.28	QSO	1.5220	2.913 ± 0.146	1.593 ± 0.159	-
1451-375	1.89	-0.37	QSO	0.3140	2.022 ± 0.101	2.026 ± 0.203	-
1453-109	1.52	0.77	QSO	0.9380	0.427 ± 0.022	0.342 ± 0.034	R
1504-166	1.98	0.16	QSO	0.8760	1.447 ± 0.073	2.334 ± 0.233	-
1508-055	2.43	0.30	QSO	1.1910	1.282 ± 0.064	0.837 ± 0.084	-
1510-089	3.08	-0.31	QSO	0.3610	2.490 ± 0.125	2.089 ± 0.209	-
1514-241	2.00	0.16	BL/GAL	0.0486	1.911 ± 0.096	2.351 ± 0.235	-
1519-273	2.35	-0.27	BL/QSO	0.0710	1.586 ± 0.080	1.140 ± 0.114	-
1524-136	1.23	0.63	QSO	1.6870	0.459 ± 0.023	0.443 ± 0.044	-
1541-828	1.47	-0.20	QSO?	–	0.589 ± 0.030	0.500 ± 0.050	-
1550-269	1.17	0.23	QSO	2.1450	0.584 ± 0.030	0.538 ± 0.054	R
1547-795	1.40	0.79	GAL	0.4830	0.150 ± 0.008	0.125 ± 0.013	R
1549-790	3.67	0.26	GAL	0.1490	1.434 ± 0.072	1.160 ± 0.116	-
1555+001	2.24	-0.34	QSO	1.7700	0.880 ± 0.044	0.688 ± 0.069	-
1602-093	1.19	0.92	GAL	0.1090	0.078 ± 0.006	0.073 ± 0.007	R
1610-771	3.91	-0.06	QSO	1.7100	2.654 ± 0.133	2.252 ± 0.225	-
1619-680	1.86	-0.07	QSO	1.3540	0.718 ± 0.036	0.581 ± 0.058	-
1622-253	2.08	0.14	QSO	0.7860	2.200 ± 0.112	0.988 ± 0.099	-
1637-771	2.87	0.56	GAL	0.0427	0.424 ± 0.021	0.503 ± 0.050	-

Table 1. Continued.

Name	$S_{5\mathrm{GHz}}$ (Jy)	$\alpha^{5}_{2.7}$	type	z	$S_{18.5\mathrm{GHz}}$ (Jy)	$S_{22\mathrm{GHz}}$ (Jy)	ext
1655-776	1.13	0.38	GAL	0.0944	0.123 ± 0.008	0.505 ± 0.051	R
1717-009	22.15	0.78	GAL	0.0304	0.150 ± 0.012	0.190 ± 0.019	R
1718-649	3.81	0.08	GAL	0.0145	3.002 ± 0.150	2.498 ± 0.250	-
1721-026	1.19	0.41	GAL	0.0330	0.020 ± 0.001	0.063 ± 0.006	R
1733-565	3.45	0.46	GAL	0.0985	0.216 ± 0.011	0.198 ± 0.020	-
1737-608	1.14	0.62	GAL?	0.3689	0.072 ± 0.004	0.061 ± 0.006	-
1741-038	3.68	-0.75	QSO	1.0570	4.873 ± 0.245	3.723 ± 0.372	-
1740-517	3.04	0.67	GAL?	0.4016	1.369 ± 0.069	1.096 ± 0.110	-
1814-637	4.48	0.75	GAL	0.0627	1.581 ± 0.079	1.383 ± 0.138	-
1815-553	1.35	0.02	QSO	–	1.088 ± 0.054	0.779 ± 0.078	-
1829-718	1.02	1.03	—	–	0.258 ± 0.013	0.197 ± 0.020	-
1831-711	1.19	0.17	QSO	1.3560	2.222 ± 0.111	1.688 ± 0.169	-
1839-486	1.30	0.68	GAL	0.1120	0.196 ± 0.010	0.093 ± 0.009	-
1903-802	1.84	-0.29	QSO	0.5000	0.615 ± 0.031	0.534 ± 0.053	-
1929-397	1.02	0.69	GAL	0.0746	0.038 ± 0.003	0.029 ± 0.003	R
1932-464	3.46	1.05	GAL	0.2310	0.507 ± 0.025	0.411 ± 0.041	R
1933-400	1.48	-0.26	QSO	0.9660	1.165 ± 0.058	1.245 ± 0.124	-
1934-638	6.26	0.96	GAL	0.1830	1.169 ± 0.059	0.813 ± 0.081	-
1936-155	1.69	-0.26	QSO	–	0.968 ± 0.049	1.118 ± 0.112	-
1938-155	2.24	0.96	GAL	0.4520	0.494 ± 0.025	0.417 ± 0.042	-
1936-623	1.10	0.16	QSO	0.6982	0.535 ± 0.027	0.512 ± 0.051	-
1954-388	2.06	-0.43	QSO	0.6260	3.800 ± 0.190	2.734 ± 0.273	-
1954-552	2.38	0.76	GAL	0.0598	0.298 ± 0.015	0.209 ± 0.021	-
1958-179	1.20	-0.13	QSO	0.6500	1.364 ± 0.069	0.800 ± 0.080	-
2000-330	1.15	-0.78	QSO	3.7770	0.516 ± 0.026	0.517 ± 0.052	-
2005-489	1.23	-0.24	BL/GAL	0.0710	1.339 ± 0.067	0.927 ± 0.093	-
2008-068	1.37	0.68	GAL	0.5470	0.401 ± 0.021	0.308 ± 0.031	R
2008-159	1.39	-1.02	QSO	1.1800	2.269 ± 0.114	1.100 ± 0.110	-
2020-575	1.08	0.71	GAL	0.3520	0.101 ± 0.005	0.072 ± 0.007	R
2032-350	1.94	0.89	GAL?	1.0682	0.395 ± 0.020	0.337 ± 0.034	-
2037-253	1.20	-0.42	QSO	1.5740	0.447 ± 0.024	0.890 ± 0.089	R
2044-027	1.02	0.52	QSO	0.9420	0.360 ± 0.019	0.296 ± 0.030	-
2053-201	1.02	0.69	GAL	0.1560	0.097 ± 0.007	0.193 ± 0.019	R
2052-474	2.52	0.11	QSO	1.4910	0.741 ± 0.037	1.441 ± 0.144	-
2058-282	2.13	0.62	GAL	0.0377	0.096 ± 0.005	0.124 ± 0.012	R
2104-256	4.55	0.73	GAL	0.0370	0.078 ± 0.004	0.087 ± 0.009	R
2106-413	2.35	-0.17	QSO	1.0547	1.891 ± 0.095	2.290 ± 0.229	-
2126-158	1.28	-0.14	QSO	3.2660	0.931 ± 0.048	0.790 ± 0.079	-
2128-123	2.07	-0.11	QSO	0.5010	3.611 ± 0.181	3.000 ± 0.300	-
2131-021	2.12	-0.13	BL/QSO	0.5570	2.244 ± 0.114	1.693 ± 0.169	-
2135-147	1.41	0.70	QSO	0.2000	0.152 ± 0.010	0.500 ± 0.050	R
2135-209	1.55	0.77	GAL	0.6350	0.451 ± 0.024	0.580 ± 0.058	-
2142-758	1.32	0.07	QSO	1.1390	0.685 ± 0.034	0.625 ± 0.062	-
2140-816	1.00	0.73	—	–	0.114 ± 0.006	0.086 ± 0.009	-
2149-287	1.36	0.61	GAL	0.4790	0.411 ± 0.021	0.410 ± 0.041	-
2150-520	1.21	0.95	QSO?	–	0.259 ± 0.013	0.193 ± 0.019	-
2152-699	12.28	0.63	GAL	0.0285	1.412 ± 0.071	1.248 ± 0.125	R
2155-152	1.77	-0.15	QSO	0.6720	2.472 ± 0.125	1.480 ± 0.148	-
2203-188	4.38	0.28	QSO	0.6190	2.197 ± 0.111	2.000 ± 0.200	-
2204-540	2.41	-0.16	QSO	1.2060	1.277 ± 0.064	1.175 ± 0.117	-
2206-237	1.01	0.45	GAL	0.0870	0.340 ± 0.017	0.284 ± 0.028	-
2210-257	1.05	-0.15	QSO	1.8330	0.604 ± 0.034	1.100 ± 0.110	-
2211-172	2.17	1.21	GAL	0.1530	0.059 ± 0.003	0.178 ± 0.018	R
2216-038	1.50	-0.48	QSO	0.9010	2.540 ± 0.128	1.818 ± 0.182	-
2221-023	2.11	0.76	GAL	0.0562	0.039 ± 0.002	0.045 ± 0.005	R
2223-052	4.51	0.11	QSO	1.4040	8.129 ± 0.407	7.253 ± 0.725	-
2226-411	1.08	0.87	QSO	0.4462	0.293 ± 0.015	0.254 ± 0.025	-

Table 1. Continued.

Name	$S_{5\mathrm{GHz}}$ (Jy)	$\alpha^{5}_{2.7}$	type	z	$S_{18.5\mathrm{GHz}}$ (Jy)	$S_{22\mathrm{GHz}}$ (Jy)	ext
2227-088	1.77	0.03	QSO	1.5610	1.618 ± 0.081	1.499 ± 0.150	-
2227-399	1.05	-0.05	QSO	0.3230	0.754 ± 0.038	0.582 ± 0.058	R
2240-260	1.03	0.08	BL/QSO	0.7740	0.573 ± 0.029	0.430 ± 0.043	R
2243-123	2.45	0.18	QSO	0.6300	2.183 ± 0.110	2.200 ± 0.220	-
2245-328	1.85	0.13	QSO	2.2550	0.164 ± 0.008	0.227 ± 0.023	R
2250-412	1.33	0.92	GAL	0.3100	0.262 ± 0.013	0.183 ± 0.018	-
2252-530	1.01	0.94	GAL?	–	0.274 ± 0.014	0.238 ± 0.024	-
2255-282	1.78	-0.41	QSO	0.9260	11.255 ± 0.563	2.250 ± 0.225	-
2311-452	1.47	0.38	QSO	2.8840	0.578 ± 0.029	0.602 ± 0.060	-
2317-277	1.30	0.64	GAL	0.1730	0.076 ± 0.004	0.045 ± 0.005	-
2323-407	1.09	0.79	GAL	0.2982	0.214 ± 0.011	0.167 ± 0.017	-
2324-023	1.16	0.49	GAL	0.1880	0.292 ± 0.016	0.278 ± 0.028	R
2326-477	2.33	0.06	QSO	1.3060	1.531 ± 0.077	1.094 ± 0.109	-
2329-162	1.06	0.06	QSO	1.1550	1.996 ± 0.100	1.044 ± 0.104	-
2331-240	1.09	-0.08	GAL	0.0477	1.151 ± 0.058	0.679 ± 0.068	-
2331-417	1.59	0.88	GAL	0.9070	0.256 ± 0.013	0.253 ± 0.025	-
2333-528	1.22	0.09	QSO	–	1.059 ± 0.053	0.946 ± 0.095	-
2337-334	1.21	0.20	QSO	1.8020	0.502 ± 0.025	0.593 ± 0.059	R
2345-167	3.66	-0.51	QSO	0.5760	2.412 ± 0.121	1.407 ± 0.141	-
2353-686	1.10	-0.26	QSO	1.7160	0.785 ± 0.039	0.502 ± 0.050	-
2354-117	1.48	0.24	QSO	0.9600	1.197 ± 0.060	0.925 ± 0.093	-
2355-534	1.52	-0.36	QSO	1.0060	1.523 ± 0.076	1.605 ± 0.161	-
2356-611	7.73	0.80	GAL	0.0958	0.060 ± 0.003	0.212 ± 0.021	R